JOURNAL OF GEOPHYSICAL RESEARCH, VOL. 103, NO. D4, PAGES 3919–3928, FEBRUARY 27, 1998

Biennial, quasi-biennial, and decadal oscillations of potential vorticity in the northern stratosphere

Mark P. Baldwin and Timothy J. Dunkerton
Northwest Research Associates, Bellevue, Washington

Abstract. Seasonal and interannual variations of the northern hemisphere stratosphere on the 600 K isentropic surface (20–35 hPa) are investigated by using observations for 1964–1996. An area diagnostic is defined in terms of Ertel's potential vorticity (PV), which measures the area enclosed by PV contours as a function of equivalent latitude and is not tied to the spherical coordinate system. Data from all seasons are examined for oscillations with periods of 6 months to more than a decade. Spectral analysis of PV at equivalent latitudes from 20°N to the pole reveals several possible signals: (1) In addition to the well-known annual cycle of the polar vortex there is a striking semiannual oscillation of PV in middle equivalent latitudes. At 34°–53°N the semiannual oscillation is larger than the annual cycle. This oscillation arises from the formation of a surf zone in winter, due to planetary wave breaking, superposed on the annual cycle. (2) A signal associated with the quasi-biennial oscillation (QBO) of the equatorial stratosphere, with average period slightly less than 30 months, is strongest at low equivalent latitudes and is apparent in middle equivalent latitudes up to 67°N. Through interaction with the annual cycle, oscillations with periods of 20.2 and 8.5 months are generated. These three spectral peaks at approximately 30, 20, and 8.5 months have been observed in ozone and wind data and are seen here, for the first time, in PV. (3) At middle to high equivalent latitudes, on the other hand, we observe biennial and associated 8-month oscillations related to the occurrence of stratospheric warmings and strong, undisturbed vortices in midwinter to late winter. The data record is remarkable in that, at high equivalent latitudes, strong and weak polar vortices alternated from year to year, producing the biennial signal and a significant negative lag-1-year autocorrelation. The addition of an 8-month harmonic generates a much better fit to the sharp late winter anomalies. (4) South of 60°N a spectral peak at 10.6 years is observed, with the clearest signal near 20°N. This spectral peak may be caused by the solar cycle, or it may arise through interaction of biennial and quasi-biennial oscillations.

1. Introduction

On timescales ranging from intraseasonal to interannual the stratospheric polar vortex is influenced by several factors: e.g., the propagation and breakdown of planetary waves originating in the troposphere, low-frequency tropospheric circulation anomalies, the seasonal cycle of diabatic heating and cooling in the stratosphere, the equatorial quasi-biennial oscillation (QBO), volcanic eruptions, El Niño/Southern Oscillation (ENSO), and decadal variations possibly associated with the solar cycle.

A concise description of the stratospheric flow and its seasonal and interannual variability can be obtained in terms of Ertel's potential vorticity (PV). In this study, we use daily maps of PV on the 600 K isentropic surface to characterize the polar vortex and to examine the data for regular and nearly regular oscillations. PV is a quasi-conservative tracer of air motion along isentropic surfaces. Following *McIntyre and Palmer* [1983, 1984], the high Richardson number approximation to Ertel's PV is used:

$$P = -g(\zeta + f)\partial\theta/\partial p$$

The relative vorticity, ζ, is computed on constant pressure surfaces, and $\partial\theta/\partial p$ is static stability. Hereafter, P is scaled by the climatological value of static stability (defined by using the lapse rate of the U.S. Standard Atmosphere, as *in Dunkerton and Delisi* [1986]), and has units s^{-1}.

McIntyre and Palmer [1983, 1984] showed that isentropic maps of Ertel's PV are a fundamental, simple, and useful way of viewing dynamical processes in the northern winter stratosphere. They showed that during winter the extratropical middle stratosphere can be divided into two regions, the "main vortex" and the "surf zone." The main vortex consists of a region of high PV inside a band of steep PV gradients, while the surrounding surf zone is characterized by relatively low PV and weak gradients.

Butchart and Remsberg [1986] showed that the seasonal evolution of the stratosphere could be visualized by plotting the fractional area of the hemisphere enclosed by PV contours. In effect, PV is rearranged to be zonally symmetric, and latitudinal variations of the vortex can be displayed as PV versus

Copyright 1998 by the American Geophysical Union.

Paper number 97JD02150.
0148-0227/98/97JD-02150$09.00

equivalent latitude. Their "area diagnostic" concisely showed the evolution of the vortex/surf zone structure for the 1978–1979 winter. The area coordinate avoids the distraction of accounting for reversible wave-mean flow interactions when the polar vortex is temporarily displaced from the pole or distorted without changing size. *Baldwin and Holton* [1988] used the area diagnostic to examine the climatology and variability of the northern stratospheric vortex for 19 winters. Similar calculations during the initial period of the Upper Atmosphere Research Satellite (UARS) were reported by *Zurek et al.* [1996].

2. Data and Processing

Our data consist of daily National Centers for Environmental Prediction (NCEP, formerly the National Meteorological Center, or NMC) 1200 UTC heights and temperatures. For the period January 1, 1964 to September 23, 1978, these data are available north of 18°N at the levels 1000, 850, 700, 500, 400, 300, 250, 200, 150, 100, 70, 50, 30, and 10 hPa. After that date the coverage became global, and the levels 5, 2, and 1 hPa were added. The data set is archived on a 5° × 4° longitude/latitude grid for the period January 1, 1964 to May 11, 1996. For this study the period May 12, 1964 to May 11, 1996 was used. Discarding the initial period (January 1, 1964 to May 11, 1964) leaves exactly 32 years of data with endpoints in late spring. By using an even number of years one of the spectral frequencies (viz., the sixteenth harmonic) corresponds to a period of exactly 2 years. The data were subject to quality control to remove erroneous grids. Single missing levels were vertically interpolated. All remaining missing data were linearly interpolated in time. Horizontal wind components were calculated by using the linear balance method [*Robinson*, 1986; *Hitchman et al.*, 1987; *Randel*, 1987].

Ertel's PV was then calculated on the 600 K potential temperature surface, typically found between 20 and 35 hPa, with lowest pressures occurring during the winter. The 600 K surface was chosen because it is near, but below, the 10 hPa uppermost data level for the early years. From daily maps of PV, *Butchart and Remsberg's* [1986] area diagnostic was calculated for the region including equivalent latitudes between 20°N and the pole. On each day the area diagnostic was computed by integrating the area inside PV contours, giving area as a function of PV value. This calculation is somewhat sensitive to the grid resolution of the data as well as the spacing of PV contours. To achieve sufficient accuracy, PV fields were interpolated, by using cubic splines, to a 2° × 1° longitude/latitude grid, and a spacing of 2.5×10^{-5} s^{-1} was used (190 contour values). The PV data were transformed onto a grid of 66 evenly spaced points in sin(equivalent colatitude) from 0.0 to 0.65, corresponding to 90.0°–20.5°N. This latitudinal coordinate is linearly proportional to area on the sphere. The result of the transformation is an array of PV values on a grid of 11,688 days by 66 equivalent latitudes. All of the calculations are based on this equivalent latitude grid. For brevity we use "latitude" to refer to "equivalent latitude." Similarly, the "pole" refers to the "equivalent north pole." Subsequently, the data were 10-day low-pass filtered. Spectral calculations were performed by sampling time series every 5 days, and 50 points at the beginning and end of each time series were linearly tapered to zero. The results are insensitive to taper width, because the endpoints are in May, a time of small interannual variability in the northern stratosphere.

For time series analysis the QBO is represented by monthly means of Singapore zonal wind at 40 hPa. The solar cycle time series consists of observed monthly mean values of 10.7-cm solar flux, smoothed with a 13-month running mean.

3. Results

A climatology of the area diagnostic was constructed by averaging over each calendar day and then smoothing the daily average with a 90-day low-pass filter (this process is equivalent to keeping about four harmonics of the annual cycle). The filter cutoff was sharp enough so that periods of 6 months and longer were nearly unaffected by the smoothing. The smoothed climatology captures the essential features of an unsmoothed climatology while eliminating noise. Figure 1a shows the climatological average of the area diagnostic for 32 years of data on the 600 K surface. For clarity, two annual cycles are shown. The dominant feature is the polar vortex (shaded for values greater than 1.3×10^{-4} s^{-1}) which develops rapidly in autumn and, on average, dissipates even more quickly in spring. This climatology presents a picture consistent with the concepts of wave breaking and vortex/surf zone regions proposed by *McIntyre and Palmer* [1983, 1984]. In their conceptual model, breaking planetary waves erode the vortex at its periphery, stripping off high-PV air and irreversibly mixing it into the surrounding surf zone (which extends southward beyond the lowest latitudes shown here). This situation contrasts with that obtained from a zonally symmetric general circulation model of the middle atmosphere [*Butchart and Remsberg*, 1986, Figure 6] in which the evolution of the vortex is nearly symmetric about a midwinter PV maximum.

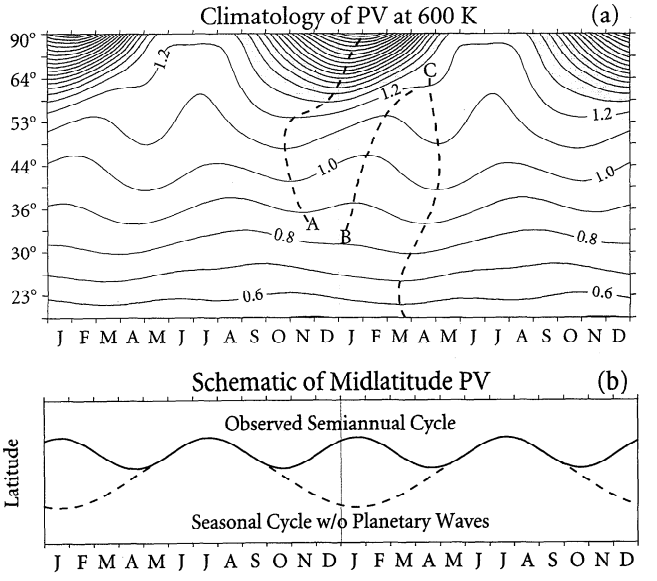

Figure 1. (a) The 32-year climatology of the potential vorticity area diagnostic on the 600 K isentropic surface, smoothed with 90-day low-pass filter. For clarity, two seasonal cycles are shown. The contour labels are scaled by 1.0×10^{4} s^{-1}. Values greater than 1.3×10^{-4} s^{-1} are shaded. The heavy dashed lines A, B, and C follow local maxima and minima; see text for details. (b) Idealized schematic illustration of midlatitude PV contours. The solid curve represents the observed PV climatology, typical of the 1.0×10^{-4} s^{-1} contour in Figure 1a. The dashed segments describe a hypothetical seasonal cycle in the absence of planetary waves.

Since the PV climatology is the average of discrete events that occur at different times for different years, the effect is to dull the distinction between the polar vortex and surrounding surf zone, but the basic features of PV evolution can be traced through the climatological seasonal cycle. In autumn, PV values increase at latitudes north of 30°N, consistent with Butchart and Remsberg's zonally symmetric model, which has virtually no annual cycle at 30°N. The increase of PV is halted in midlatitudes during late October and early November. Butchart and Remsberg's data for the 1978–1979 winter (their Figure 4) show essentially the same feature. During autumn, upward propagating planetary waves are not focused into the polar cap but begin to define the vortex edge at lower latitudes by mixing PV there, subsequently involving higher PV contours at higher latitudes as the winter season progresses. Figure 4 of *Butchart and Remsberg* [1986] clearly shows how, during late autumn, the outer edge of the region of tight PV gradients initially defines the vortex boundary at low latitudes and the boundary is found at successively higher values of PV at later times. At the edge of the shaded region the vortex has already begun shrinking during December, but at the center of the vortex the highest PV values are not attained until early February.

In Figure 1a the heavy dashed line A traces the time at which PV values stop increasing at each equivalent latitude. The region between lines A and B defines the period in which midlatitude PV decreases with time. This process may be seen as a tightening of PV gradients at the vortex edge in Butchart and Remsberg's data for the 1978–1979 winter and in other years shown by *Baldwin and Holton* [1988]. In midlatitudes the process of wave breaking and vortex erosion substantially alters the predominantly annual cycle that would be observed in a zonally symmetric atmosphere. *Butchart and Remsberg's* [1986] Figure 7 illustrates the mean PV value between 20°N and the pole for both the real atmosphere and a zonally symmetric model. They concluded that the effect of planetary waves is to reduce the average PV north of 20°N after the vortex is established in autumn. In individual years this process is not necessarily continuous, as is implied by the climatology, but intermittent. Each wave breaking episode reduces the average PV, presumably by mixing with the region south of 20°N. Diabatic effects attempt to restore the PV distribution to an undisturbed state. Potential vorticity increases with time between B and C, and at lower latitudes the very gradual increase of PV beginning in autumn ends along line C.

The entire region between lines A and C may be interpreted as an effect of breaking planetary waves which act initially to reduce PV values during the erosion process. Before and after this period the midlatitude region is much closer to an axisymmetric structure simulated in the absence of planetary waves. A striking result of the erosion process may be seen near 45°N on the $1.0 \times 10^{-4}s^{-1}$ contour. Instead of an annual cycle in PV, the dominant component is a semiannual cycle, produced by the signature of vortex erosion superposed on the annual cycle. This concept is illustrated schematically in Figure 1b, showing the observed semiannual cycle of the 1.0×10^{-4} s^{-1} contour from Figure 1a and an annual cycle that would presumably occur in the absence of waves. In this schematic, formation of the surf zone decreases PV values during midwinter. Outside this time period the distribution of PV is near its undisturbed state. We note, however, that in Figure 1a the timing of largest deviation from an annual cycle depends on latitude, with maximum deviations occurring later for higher PV contours.

The effect of planetary waves is not restricted to surf zone breaking and erosion, since the dynamical transport of these waves also maintains a departure from radiative equilibrium at the winter pole and induces a mean meridional circulation of global scale. Such effects are implicit in the temporal evolution of potential vorticity, but a detailed analysis of the PV balance is beyond the scope of this paper. One feature, highlighted in a recent paper by *Dunkerton and O'Sullivan* [1996], is the formation of a detached subtropical jet in late northern winter. This feature is evident in Figure 1a as a band of enhanced PV gradient, which might otherwise be interpreted as a region of suppressed lateral mixing. Although mixing is indeed suppressed here, the formation of the jet in the first place involves westerly accelerations that cannot be attributed solely to Rossby wave drag.

Time series of the area diagnostic at each equivalent latitude were examined for regular or quasi-regular oscillations. Potential vorticity time series at representative latitudes are shown in Figure 2. For clarity the time series were 90-day low-pass filtered and deseasoned (by subtracting the climatology). Deviations north of 62°N are much larger than those to the south. The largest deviations at northern latitudes occur during winter and early spring (the vertical lines indicate each January 1). Large positive and negative deviations are common. Low wintertime PV values in high latitudes tend to be mirrored as high values at lower latitudes (e.g., January 1969) and vice versa (e.g., January 1996). At low latitudes after 1980 the QBO is easily seen.

Figure 3 illustrates the resulting power spectrum at 17 equivalent latitudes (every fourth value) for periods of 5 months and greater. For this calculation the data were 10-day low-pass filtered but not deseasoned, and for clarity, individual spectra were normalized to the same maximum value. At high latitudes the annual cycle of the polar vortex is dominant and can be seen at other latitudes as well. There is, however, a minimum near 40°–50°N where the annual cycle is small. As suggested by Figure 1, the semiannual period dominates in midlatitudes. Note that the spectral power is not concentrated at exactly 12 and 6 months but also involves adjacent spectral points (e.g., 11.6 and 12.4 months). The addition of adjacent harmonics allows for low-frequency modulation of the annual and semiannual cycles. At the lowest latitudes a 29.5-month (QBO period) oscillation has more spectral power than either the annual or semiannual cycles.

To examine the data for oscillations other than the large annual and semiannual cycles, the climatology shown in Figure 1a was subtracted from the daily values of area diagnostic. By removing the annual cycle, spectral power at 12- and 6-month periods is reduced to near zero. However, moderate spectral power can remain at periods very close to the annual cycle. To eliminate the annual spectral band in its entirety, the data were notch filtered at 11–13 months by using a narrow band-pass filter. As is shown in Figure 4, most of the remaining spectral power is found at frequencies associated with a biennial oscillation, the QBO, and a decadal oscillation. Each of these oscillations and the associated spectral peaks is discussed below.

3.1. Quasi-Biennial Oscillation and Related Harmonics

As was noted by *Gray and Dunkerton* [1990], the interaction of the annual and QBO frequencies can generate new har-

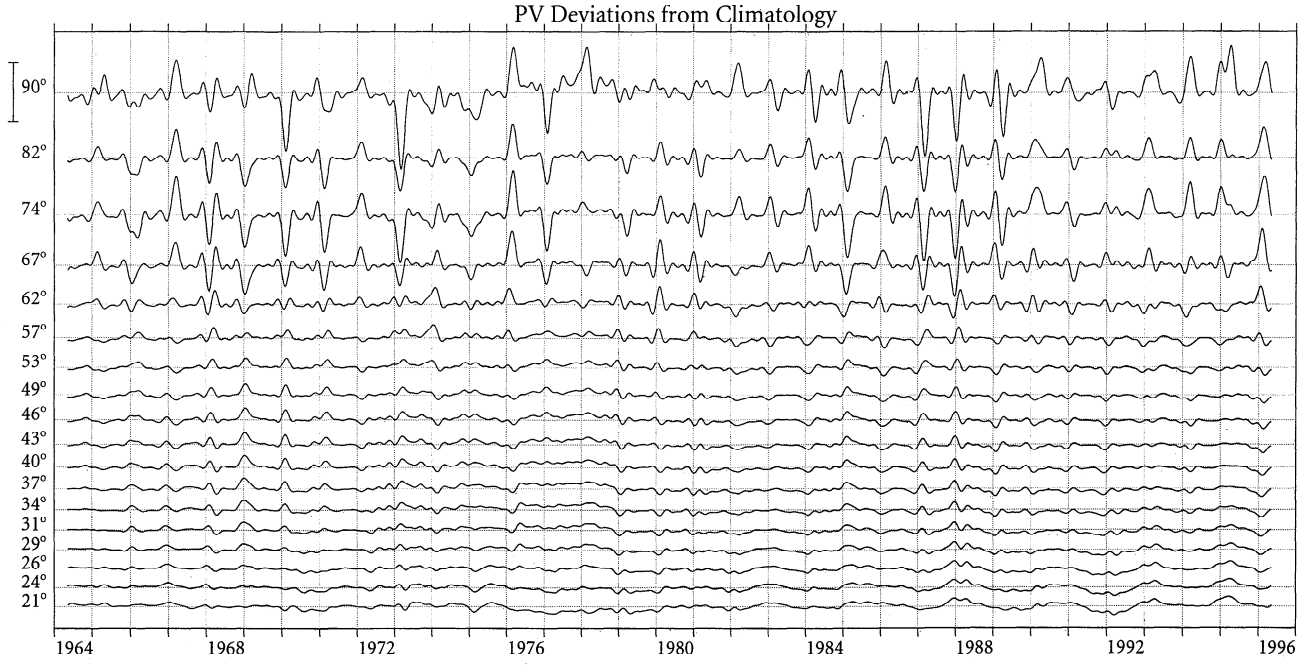

Figure 2. Time series of PV at equivalent latitudes from 21° to 90°N. The data were deseasoned by subtracting the climatology of Figure 1a and were smoothed with a 90-day low-pass filter. The vertical axis is linear in sin(equivalent colatitude) and the vertical scale is the same for all equivalent latitudes. The scale bar at the left edge of the figure indicates a range of 1.0×10^{-4} s^{-1}.

monics with frequencies equal to their sum or difference. In spectra of ozone [*Tung and Yang*, 1994a], angular momentum, and Eliassen-Palm (EP) flux divergence [*Baldwin and Tung*, 1994] the QBO was found to exhibit a three-peak (~30-, 20-, and 8.6-month periods) spectrum through its interaction with the annual cycle.

The period of the QBO varies, averaging 28.7 months during 1964–1995. The best fit to the Singapore 40-hPa wind is obtained with a 28.7-month harmonic (yielding a correlation of 0.71). However, no single harmonic can fit the QBO's variable period. In a 32-year data set the closest discrete harmonics to the QBO are at 32.0, 29.5, and 27.4 months. The power spectrum of Singapore 40-hPa zonal wind is shown in Figure 6a and is essentially the same as that shown by *Tung and Yang* [1994a] for Singapore 30-hPa wind. There is modest power at 32 months, with a peak at 29.5, and nearly as much power at 27.4 months.

In Figure 4 the three-peak spectrum of the QBO can be seen in potential vorticity. The 29.5-month peak is clearly visible at most latitudes south of 67°N but is weak at the pole. The 20.2-month peak is evident south of 53°N, and the 8.5-month peak is present between 57° and 67°N.

A complementary view of the spectral peaks is obtained by correlating the PV area diagnostic at each equivalent latitude with best fit harmonics having periods identical to those used in the spectral analysis. Each best fit harmonic is obtained by retaining only a single sinusoidal harmonic (e.g., 24 months) from the PV data at each equivalent latitude. Figure 5 illustrates these correlations, which tend to accent regions of low total variance (e.g., low latitudes) while suppressing regions of high variance such as the north pole. The 29.5- and 20.2-month peaks are clearly visible, while an 8.5-month correlation is present but not well defined. This diagram reinforces the view obtained from spectral analysis. In general, correlations greater than 0.10 seem to correspond to the spectral peaks visible in Figure 4. Peak correlations south of 30°N for the 29.5-month harmonic exceed 0.45, while correlations above 0.10 extend north to 67°N. The latitudinal extent of the 20.2-month harmonic in Figure 5 is similar to that of the spectra in Figure 4; there is a band of correlations greater than 0.10 extending over the subtropics and midlatitudes. Correlations with the 8.5-month harmonic exceed 0.10 only near 65°–75°N. The latitudes of maximum 29.5- and 20.2-month correlation are similar, while the 8.5-month correlation is observed only in the northernmost range of the 29.5-month harmonic. Thus the regions affected by the 20.2- and 8.5-month oscillations are distinct in the correlation plot.

To explore further the 29.5- and 20.2-month oscillations, the time series at 23°N was filtered to include only the QBO frequency band. The data were reconstructed with a narrow 1-2-1 band-pass filter, retaining the central harmonic (in this case, 29.5 months) plus half the adjacent harmonics (32.0 and 27.4 months). Figure 6b illustrates these narrow band-pass data in comparison with 90-day low-pass-filtered, deseasoned data and monthly mean Singapore 40-hPa zonal wind. The inclusion of harmonics adjacent to 29.5 months allows some variation of the amplitude of the signal, with the greatest amplitude obtained during the 1980s. Comparison of the data with the reconstructed (gray) curve shows that the best fit is obtained during the later years. The poor fit in early years results from the variable period of the QBO and the smaller amplitude of the QBO resolved by NCEP data during this time. Until about 1980 the amplitude of the QBO in PV is small but discernible. In the second half of the data set it is prominent. The change in character of the data coincides with the use of satellites for operational NCEP data in the late 1970s. Com-

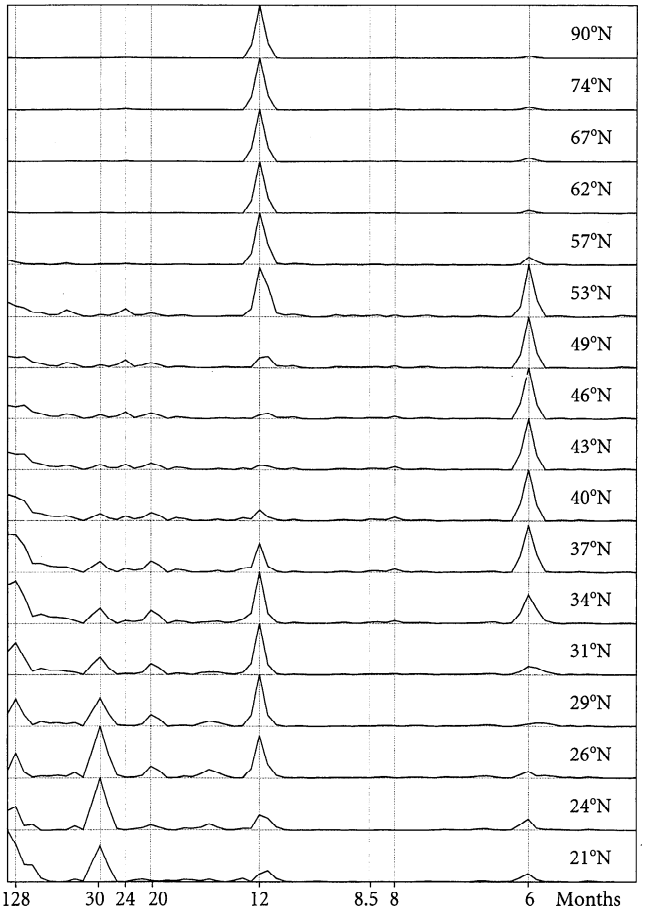

Figure 3. Power spectra of PV at equivalent latitudes from 21° to 90°N. Vertical gray lines indicate 128-, 29.5-, 24.0-, 20.2-, 8.53-, 8.0-, and 6.0-month periods. The vertical scale for each time was adjusted so that the maximum value at each latitude is the same.

paring the Singapore 40-hPa wind to the PV data shows a reasonable match of maxima and minima (the correlation between Singapore wind and PV at 23°N is 0.46 for the first 16 years and 0.60 for the second 16 years). The gray curve superposed on the Singapore wind is a reconstruction of the Singapore wind using a 1-2-1 filter centered on 29.5 months. The reconstruction does not provide a good fit during all years because the period of the reconstructed curve is so narrowly defined. The poor fit during early years can also be traced to 1972–1976 when the QBO period was 24 months.

In Figure 6c the solid curve is a reconstruction using the same method as that in Figure 6b, except that the 20.2-month band is added (again using 1-2-1 weighting surrounding the central harmonic). The correlation is increased only modestly from 0.65 to 0.70. In Figure 6d an improved fit has been obtained by dividing the record into two parts, retaining the 30- and 20.2-month spectral bands. The correlations for the respective periods are 0.46 and 0.73.

3.2. Biennial Oscillation and Related Harmonics

A spectral peak at 24 months is prominent in the power spectra (Figure 4) north of 66°N and also from 37° to 57°N. This peak is negligible at intermediate latitudes with a node at 62°N. Correlations of best fit harmonics with the data (Figure 5) show values of at least 0.10 over the entire range of latitudes except for a minimum near 62°N. A purely biennial oscillation, when modulated by the annual cycle, is expected to produce a third oscillation with a period of 8 months, in a manner similar to the three-peak QBO. In Figure 5 the 8-month spectral peak is pronounced only between 53° and 67°N and appears weakly in midlatitudes. A biennial oscillation was noted in singular spectrum analysis of the first (latitude-height) empirical orthogonal function (EOF) of northern hemisphere stratospheric temperature by *Dunkerton and Baldwin* [1992], while *Salby* [1995] and *Salby et al.* [1997] found a biennial spectral peak in 30-hPa north polar temperatures.

To examine the fit of a 24-month oscillation to high-latitude PV, data at 79°N were reconstructed by using the method in Figure 6, but with harmonics centered at 24 months (Figure 7a). The deseasoned PV shows only modest deviations from climatology except during the time period late December through April. The large deviations may be either positive (representing exceptionally strong vortices in cold, undisturbed years) or negative (representing major warmings). Examining these late winter anomalies in all years reveals that many of the spikes align with the reconstructed curve (gray line), especially in 1971–1991. The earlier and later years tend neither to contribute to this effect nor to oppose it. The reconstructed curve reflects this tendency, with a larger amplitude during the middle years. On average, the extrema in the

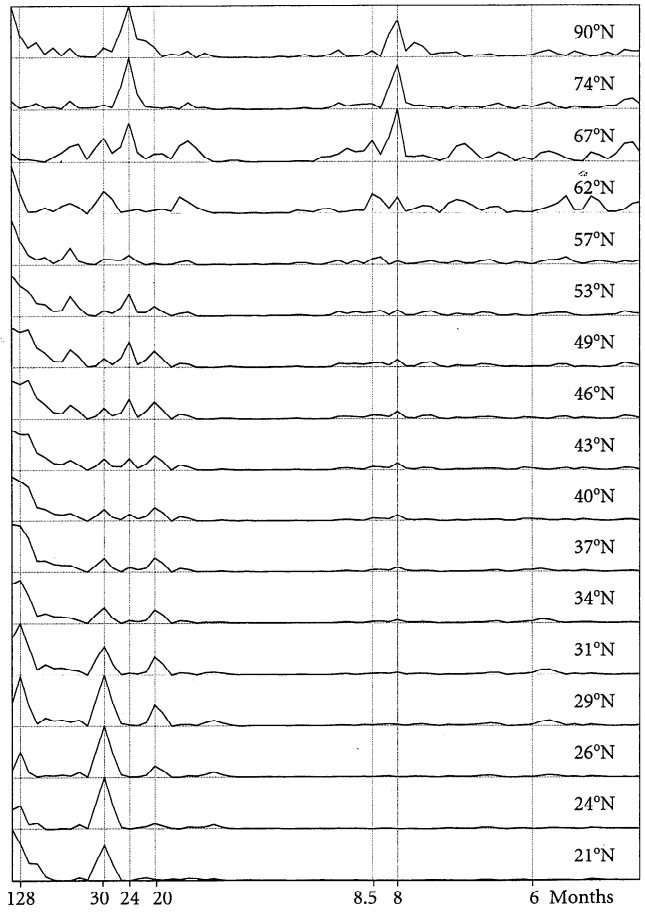

Figure 4. As in Figure 3, but for deseasoned data obtained by subtracting the climatology of Figure 1a and notch filtered to remove the 11- to 13-month band.

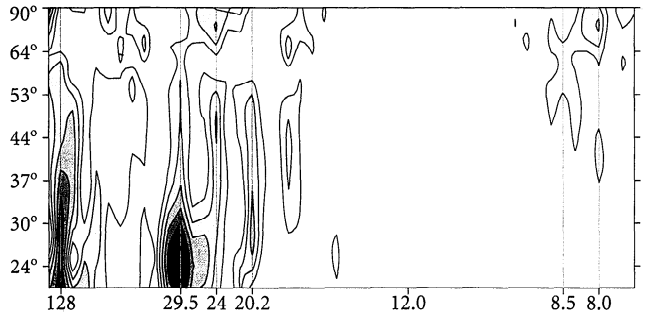

Figure 5. Correlation between PV time series and best fit harmonics. For each period the best fit harmonics are calculated by using a single sinusoidal harmonic that retains only that period (e.g., 24 months). The contour interval is 0.1, and the minimum contour is 0.1. Prior to the calculation, PV data at each equivalent latitude were deseasoned (by subtracting the climatology) and smoothed with a 10-day low-pass filter.

reconstructed curve are located in late February, coinciding with the maximum climatological variance in PV (not shown). The correlation between the reconstructed curve and the 90-day low-pass-filtered data is 0.33.

At high latitudes in Figures 4 and 5, both 24- and 8-month peaks are prominent. Figure 7b shows a reconstruction of the data at 79°N using both 24- and 8-month oscillations. The amplitude and phase of the 8-month oscillation are such that the 8-month harmonic adds constructively to the 24-month extrema and sharpens the fit to the late winter anomalies. The correlation with the data improves from 0.33 to 0.45 with the addition of the 8-month harmonic.

Since the biennial oscillation is nearly as prominent in midlatitudes, the same curve fit was performed for data at 48°N (Figure 7c). Here the amplitude of PV anomalies is much smaller (the vertical scale in Figure 7c is only 15% of that in Figure 7b), and late winter anomalies are less distinct. There are several years in which the sign of the anomaly does not change sign from the previous year. However, during each year the midlatitude anomalies tend to be of opposite sign to the polar anomalies. The correlation between time series at 48°N and 79°N is -0.56. The reconstructed curve in Figure 7c is almost exactly out of phase with that of Figure 7a. The negative correlation between high latitudes and midlatitudes represents a compensating effect consistent with McIntyre and Palmer's vortex/surf zone conceptual model as well as Butchart and Remsberg's observation that as high-PV air is mixed out of the vortex, PV values in the surf zone increase.

To isolate the nature and timing of the biennial signal, PV data for the north pole were high-pass filtered to remove low-frequency variability with timescales longer than the QBO and smoothed with a 3-month running mean. Figure 8a shows the resulting time series, with vertical lines on each January 1. Although some winter/spring periods have both positive and negative anomalies (which tend to cancel), typically each period can be represented by the 90-day mean centered on March 1. Not all winters match the alternating biennial pattern, but most of the large anomalies fit a pattern of strong vortices during even years and weak vortices during odd years. Of the 26 winters displaying a large PV anomaly in excess of about 2×10^{-5} in Figure 7a, most even years contained a large positive anomaly (strong vortex) in midwinter or late winter, while most odd years contained a large negative anomaly (weak vortex) in midwinter or late winter.

To illustrate the importance of late winter anomalies, the PV values from Figure 8a (90-day means centered on March 1) were used to construct annual spikes with 90-day width centered on March 1 (Figure 8b). Data outside each 90-day interval were set to zero. The resulting power spectrum (Figure 8c) shows pronounced 24- and 8-month peaks and looks very similar to the 90°N panel in Figure 4. Smaller spectral peaks

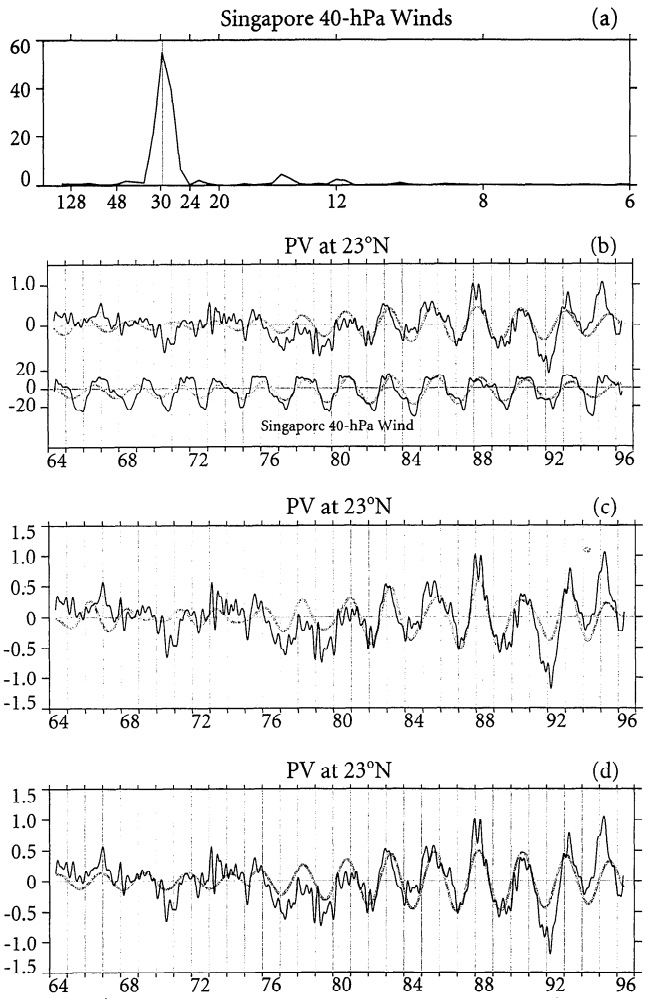

Figure 6. (a) Power spectrum of monthly mean Singapore 40-hPa wind. The vertical gray line indicates a 29.5-month period. (b) The 90-day low-pass filtered PV at 23°N (solid line) and reconstruction of the data using a 1-2-1 weighted spectral band centered on the 29.5-month harmonic (gray line). The vertical gray lines indicate January 1 of each year (1964–1996). The PV labels on the vertical axis are scaled by 10^5. The correlation coefficient between the two series is 0.65. The lower curve is the observed monthly mean Singapore 40-hPa wind, and the gray curve is a reconstruction using a 1-2-1 weighted spectral band centered on the 29.5-month harmonic. (c) The 90-day low-pass filtered PV at 23°N (solid line) and reconstruction of the data using 1-2-1 weighted spectral bands centered on both 29.5- and 20.2-month harmonics (gray line). The labels on the vertical axis are scaled by 10^5. The correlation is 0.70. (d) As is Figure 6c, but with reconstructions performed separately for 1964–1975 and 1975–1996. The correlations for the respective periods are 0.46 and 0.73.

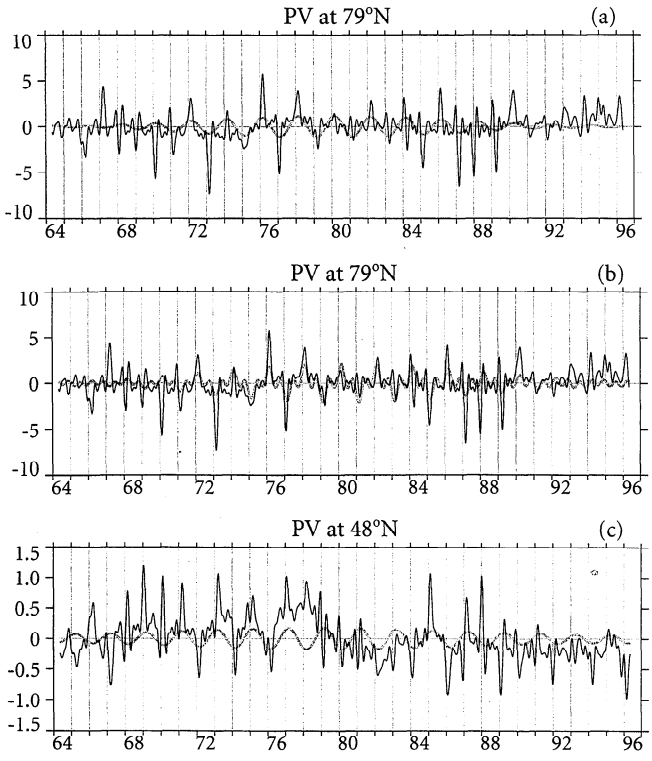

Figure 7. (a) The 90-day low-pass PV at 79°N (solid line) and reconstruction using a single 1-2-1 weighted spectral band centered on the 24-month harmonic (gray line). The vertical lines indicate January 1 of each year (1964–1996). The labels on the vertical axis are scaled by 10^5. The correlation coefficient between the two series is 0.33. (b) As in Figure 7a, but with 8.0-month band included. The correlation is 0.45. (c) As in Figure 7a except at 48°N. The correlation coefficient is 0.24.

associated with the QBO (29.5, 20.2, and 8.5 months) are also evident, and the spectrum is symmetric about 12 months.

How unusual is the biennial spectral peak seen in the high-latitude PV data? To estimate the probability of the biennial oscillation occurring by chance, we first created, for each equivalent latitude, a time series of 3-month running means centered on March 1. From these time series we obtained values of the biennial spectral power at each equivalent latitude. We then performed two Monte Carlo tests. In the first test we assumed that the annual observations are independent, and we simulated the time series with random normal deviates. Using 10,000 time series, we obtained a distribution of biennial spectral power that can be expected if the annually sampled data are independent. We found that the biennial spectral peak observed for equivalent latitudes 68°–74°N can be expected by chance less than 1% of the time.

However, the data are not independent. The lag-1-year autocorrelation of the PV data within the polar cap is negative, ranging from -0.22 to -0.37. We performed a Monte Carlo test similar to that described above, but we constrained the random time series to have a lag-one-year autocorrelation between -0.25 and -0.35. With this constraint it is easier to obtain strong biennial variability; the biennial spectral peak between 67° and 76°N can be expected by chance less than 5% of the time.

A strong autocorrelation is a necessary, but not sufficient, condition to produce a biennial spectral peak. For example, a very high autocorrelation would result from an alternating pattern in 16 winters, skipping one winter, then alternating in 15 winters again. Because the phase of the biennial oscillation in this hypothetical example switches sign in the center of the time series, the biennial power is near zero when calculated over the entire record at once, but the lag-1-year autocorrelation remains significantly negative. Since there is nothing special about even or odd years as far as the atmosphere is concerned, the more significant aspect of our north polar obser-

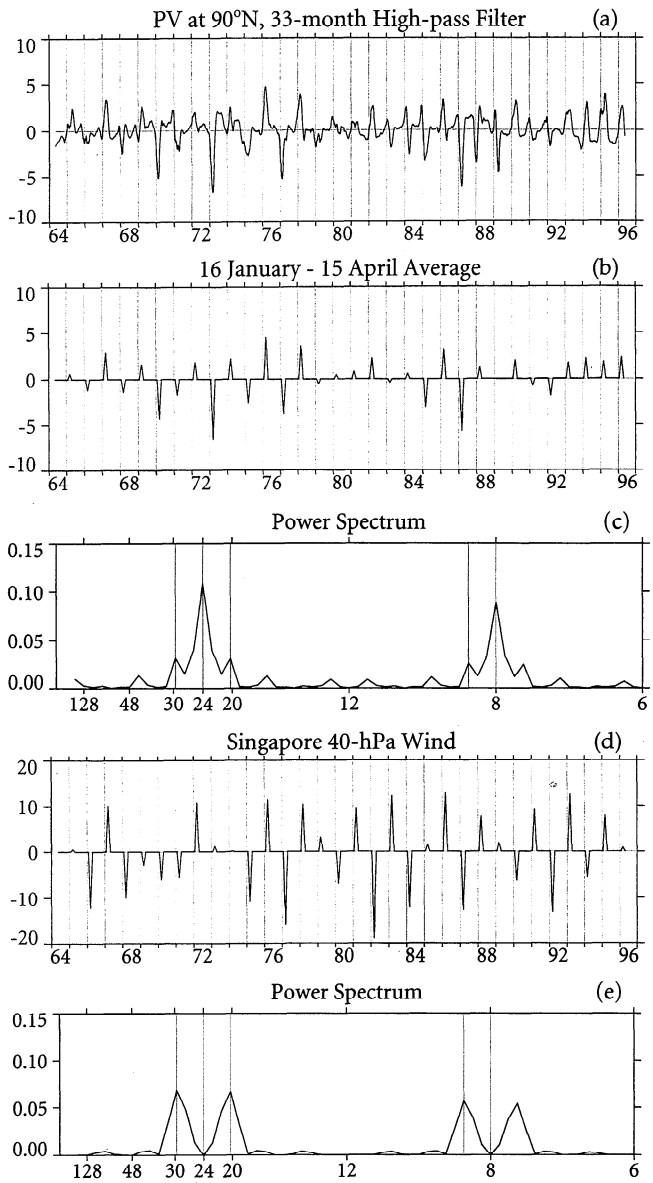

Figure 8. (a) PV time series at 90°N equivalent latitude, high-pass filtered to include periods of less than 33 months and smoothed with a 3-month running mean. The vertical lines indicate January 1 of each year (1964–1996). Labels on the vertical axis are scaled by 10^5. (b) The value on each March 1 (January 16 to April 15 average) taken from Figure 8a, defining a 90-day spike. Data are set to zero at all other times. (c) Power spectrum obtained from north polar PV in Figure 8b. The time series was normalized to unit variance. (d) As in Figure 8b, but with data values taken from a 90-day running mean of Singapore 40-hPa wind centered on March 1. (e) Power spectrum obtained from annually sampled Singapore wind in Figure 8d.

vations is the large negative lag-1-year autocorrelation and accompanying tendency for vortex anomalies to alternate sign from one year to the next. This behavior can produce biennial power during relatively short time periods.

If we substitute the spikes in Figure 8b with 90-day running mean Singapore 40-hPa wind data (sampled on March 1) and repeat the analysis, the spectral signature shows only peaks on either side of 24 and 8 months (Figures 8d and 8e); biennial power is negligible. Evidently, something in addition to the equatorial QBO is responsible for PV variability in late winter at high latitudes. Since we are not aware of any mechanism that could link even-numbered years decades apart, we cannot rule out the possibility that the persistence of the biennial signal is largely due to chance and that it is a feature of this particular data record. It was shown by *Dunkerton and Baldwin* [1992] that in February the north polar temperature in the lower stratosphere is correlated not with the QBO per se, but with a modulated signal consisting of the product of a decadal time series and sign of the QBO (*Labitzke and van Loon*, 1988). The influence of the QBO on north polar temperature in late winter varies on a decadal timescale. It was also shown empirically by *Dunkerton and Baldwin* [1992] that a biennial time series, acting in combination with quasi-biennial variations, could produce the observed decadal modulation.

3.3. Decadal Oscillation

At latitudes south of 60°N in Figure 4 a spectral peak centered broadly on 128 months (10.6 years) emerges, suggestive of the 11-year solar cycle. A solar cycle signal in the stratosphere would be expected at low, rather than high, latitudes as a result of solar heating effects. *Van Loon and Labitzke* [1990] found that midlatitude to low-latitude geopotential variability at 30 hPa correlated well with the solar cycle during all months of the year. The relationship between PV at 20°N and the observed 10.7 cm solar flux is shown in Figure 9a. The correlation of PV data with the solar flux is -0.24 and is compromised somewhat by the large-amplitude QBO in the second half of the data. A slightly better correlation (-0.35) is obtained if the PV data are lagged by 1 year. The lower solid curve in Figure 9a is a reconstruction using the 128-month band, yielding a correlation of 0.52. Although low-latitude PV varies on a decadal timescale, its relation to the solar cycle is less convincing, especially considering that the data record includes only three solar cycles.

Figure 9b shows the power spectrum of the solar 10.7-cm flux time series. Although a spectral peak appears at 128 months, there is considerable power at adjacent periods (192 and 96 months). This spectrum looks similar to that of PV at latitudes south of 35°N (Figure 4).

As an alternative to the solar cycle hypothesis we note the possibility that the observed 128-month spectral peak may be the result of interaction between quasi-biennial and biennial oscillations, in the same way that an annually modulated QBO produces 20.2- and 8.6-month peaks. For a "QBO × biennial" oscillation, the resulting spectral peaks occur at 128 and 13 months. Figure 9c illustrates the power spectrum resulting from the QBO (reconstructed by using a 1-2-1 weighting of the frequencies centered on 29.5 months) multiplied by a purely biennial sinusoidal harmonic. The power spectrum shows peaks at both 13 and 128 months. In the data a 13-month peak would be difficult to extract, since it would probably be weak in comparison with the annual cycle.

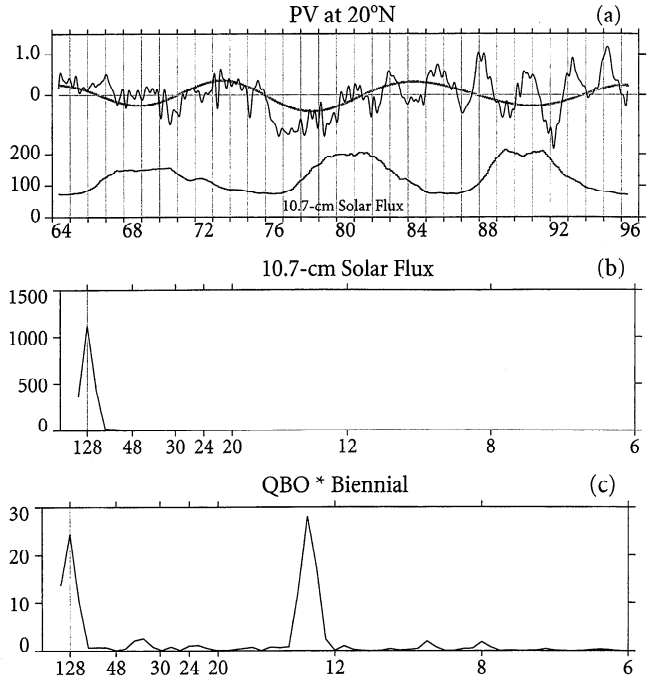

Figure 9. (a) The 90-day low-pass filtered PV at 20°N (solid line) and reconstruction of the data using a 1-2-1 weighted spectral band centered on the 128.5-month harmonic (gray curve). The vertical lines indicate January 1 of each year (1964–1996). Labels on the vertical axis are scaled by 10^5. The correlation coefficient between the two series is 0.65. The lower curve is a 13-month running mean of observed 10.7-cm solar flux. (b) Power spectrum of solar flux. (c) Power spectrum of the product of a biennial sinusoid and observed quasi-biennial signals.

If the 128-month peak results from interaction between the QBO and biennial components, one might expect the decadal variation to be found where both the QBO and biennial components are seen. Figure 6 shows that this is generally true. The QBO is visible from 20° to 67°N, while the biennial component is seen from 20° to 58°N and again north of 64°N. The location and size of the correlations for the 128-month harmonic are similar to those of the QBO. The 24-month harmonic overlaps this latitudinal band but is strongest in midlatitudes and high latitudes.

4. Conclusion

Spectral and correlation analysis of a PV area diagnostic for 32 years of data on the 600 K isentropic surface reveal annual and semiannual cycles, a biennial oscillation, a quasi-biennial oscillation, and a decadal oscillation similar to the solar cycle. Additional harmonics result from modulation of biennial and quasi-biennial oscillations by the annual cycle. It is remarkable that the data show few other spectral peaks or noise. The PV area diagnostic provides a powerful tool, averaging data along PV contours rather than latitude circles. As was shown by *Butchart and Remsberg* [1986], a clearer picture of the dynamics is obtained.

At high latitudes the annual cycle is the dominant mode of variability, representing the annual formation and dissipation of the polar vortex. In midlatitudes a semiannual oscillation is more pronounced. The semiannual oscillation arises from the

formation and dissipation of a vortex/surf zone structure, superposed on the annual cycle. This process, due to breaking planetary waves, causes a wintertime reversal of the formation of moderately high PV that would be expected in the absence of planetary waves and their attendant erosion of the polar vortex. Although a double annual temperature maximum has been observed, due to summer solar heating and winter wave driving of poleward and downward flow, this is the first observation of a semiannual cycle in PV.

Extratropical effects of the equatorial QBO have been observed [*Holton and Tan*, 1980, 1982; *Dunkerton and Baldwin*, 1991; *Baldwin and Dunkerton*, 1991] and modeled [*O'Sullivan and Dunkerton*, 1994] to occur during the extended winter season. A preference for winter is consistent with the hypothesis that quasi-stationary planetary waves, which propagate vertically only at this time of year, are essential to the QBO's influence on the polar vortex. As a result the QBO signal in extratropical latitudes is modulated by the annual cycle to produce 20-month and 8.5-month harmonics, as found by *Tung and Yang* [1994a, b] and *Baldwin and Tung* [1994] who observed a three-peak QBO spectrum in ozone and angular momentum, respectively, using data from all seasons. Seasonal synchronization is also observed in the subtropical ozone QBO, as was noted by *Gray and Dunkerton* [1990] and others. Our PV area diagnostic confirms the three-peak QBO signature for the region outside the polar vortex. The QBO is seen up to approximately 67°N, but only weakly at the pole, possibly as a result of the large variance there. A related 20.2-month signal is also seen over nearly the same latitudes, while an 8.5-month signal is observed only in the range 57°–67°N. At low latitudes the QBO spectral peak is stronger than the annual cycle.

The existence of a biennial polar oscillation is not well documented but has been noted in an EOF analysis of zonal mean stratospheric temperature by *Dunkerton and Baldwin* [1992] and in north pole temperature by *Salby* [1995] and *Salby et al.* [1997]. A biennial oscillation of PV is found at high latitudes and in midlatitudes with opposite phase. An 8-month oscillation is seen at similar latitudes, generated through interaction of 24- and 12-month signals. These spectral peaks describe well the late winter anomalies of PV, representing the signatures of major warmings and, in the opposite sense, strong vortices in cold, undisturbed winters.

The interannual variability of PV in the polar cap is well represented by 3-month means centered on March 1. If the 32 years of observations are assumed to be independent, the biennial spectral peak can be expected to occur by chance less than 1% of the time. However, the state of the polar vortex does not appear to be independent of the previous year's state. The lag-1-year autocorrelation within the polar vortex is near -0.3 and likely reflects the influence of the QBO, which usually changes sign from year to year. If the lag-1-year autocorrelation is assumed to be -0.3, the probability of obtaining the observed biennial spectral peak is slightly less than 5% within the polar cap. Beyond the influence of the QBO, which is incapable of generating a purely biennial signal, there exists the possibility that the subtropical flow anomalies persist long enough to influence the formation of the polar vortex during the following autumn and winter.

An intriguing possibility for the maintenance of a biennial signal was suggested recently by R.K. Scott and P.H. Haynes (Internal variability of the extratropical stratospheric circulation: The interannual flywheel, submitted to *Quarterly Journal of the Royal Meteorological Society*, 1997). In a mechanistic primitive equation model of the stratosphere they note the possibility that zonal wind anomalies in the subtropics can persist through the summer and affect the formation of the polar vortex during the following autumn, in a manner similar to the extratropical influence of the QBO. In their model a biennial oscillation is observed, even with no interannual variability in wave forcing or imposed QBO. In preliminary calculations with observational data we find that at low latitudes to midlatitudes, 600-K PV during the summer and autumn is positively correlated with values from the previous winter, consistent with the idea that winter anomalies may persist long enough to affect the development of the vortex during the following autumn and winter. However, the effect is difficult to distinguish from that of the QBO.

Finally, a decadal spectral peak is apparent, especially at low latitudes, where stratospheric ozone heating is modulated by the solar cycle [*Haigh*, 1996]. The observed 128-month component of PV at 20°N shows reasonable agreement with the solar 10.7-cm flux time series; a better fit is obtained when the solar cycle leads the data by almost 1 year. An alternative explanation for the 128-month oscillation is that it arises through interaction of QBO and biennial modes. Such an interaction can produce spectral power at 128 months. The latitudes at which the quasi-biennial, biennial, and decadal oscillations occur are similar, although biennial power is found mainly at mid- to high latitudes. By similar reasoning a biennial signal can be produced through interaction of quasi-biennial and decadal signals.

This study was conducted by using operational NCEP analyses. There have been numerous changes over the decades in the quantity of input data and analysis schemes. In recognition of these inconsistencies the NCEP data are now being reanalyzed with a single, consistent method. The use of the reanalyzed data could significantly affect some of the results shown here, for example, the magnitude of a low-latitude QBO signal, which is clear only after satellite observations began during the 1970s. It is also possible that some of the observed low-frequency variability at all latitudes originates from changes in the input data (depending, for example, on whether satellite data were available) and analysis scheme. Further investigation of interannual variability in the reanalyzed data is therefore desirable.

The present study did not address possible tropospheric forcing. *Baldwin et al.* [1994] found that a tropospheric mode related to the North Atlantic Oscillation was strongly linked to stratospheric wind and geopotential. In preliminary work we find that a similar tropospheric mode can account for much of the polar variability after the regular oscillations have been removed. However, this mode does not exhibit a biennial spectral peak, and further study is warranted.

Acknowledgments. We thank Steve Pawson for helpful comments on the manuscript. This research was supported by the National Science Foundation, grants ATM-9303068, ATM-9405448, ATM-9500613, and ATM-9708026, and by the National Aeronautics and Space Administration, contract NASW-4844.

References

Baldwin, M.P., and T.J. Dunkerton, Quasi-biennial oscillation above 10 mb, *Geophys. Res. Lett.*, *18*, 1205–1208, 1991.

Baldwin, M.P., and J.R. Holton, Climatology of the stratospheric polar

vortex and planetary wave breaking, *J. Atmos. Sci., 45*, 1123–1142, 1988.

Baldwin, M.P., and K.-K. Tung, Extra-tropical QBO signals in angular momentum and wave forcing, *Geophys. Res. Lett., 21*, 2717–2720, 1994.

Baldwin, M.P., X. Cheng, and T.J. Dunkerton, Observed correlation between winter-mean tropospheric and stratospheric anomalies, *Geophys. Res. Lett., 21*, 114–1144, 1994.

Butchart, N., and E.E. Remsberg, The area of the stratospheric polar vortex as a diagnostic for tracer transport on an isentropic surface, *J. Atmos. Sci., 43*, 1319–1339, 1986.

Dunkerton, T.J., and M.P. Baldwin, Quasi-biennial modulation of planetary-wave fluxes in the Northern Hemisphere winter, *J. Atmos. Sci, 48*, 1043–1061, 1991.

Dunkerton, T.J., and M.P. Baldwin, Modes of interannual variability in the stratosphere, *Geophys. Res. Lett., 19*, 49–52, 1992.

Dunkerton, T.J., and D.P. Delisi, Evolution of potential vorticity in the winter stratosphere of January–February 1979, *J. Geophys. Res., 91*, 1199–1208, 1986.

Dunkerton, T.J., and D.J. O'Sullivan, Mixing zone in the tropical stratosphere above 10 mb, *Geophys. Res. Lett., 23*, 2497-2500, 1996.

Gray, L.J., and T.J. Dunkerton, The role of the seasonal cycle in the quasi-biennial oscillation of ozone, *J. Atmos. Sci., 47*, 2429–2452, 1990.

Haigh, J.D., The impact of solar variability on climate, *Science*, 272, 981–984, 1996.

Hitchman, M.H., C.B. Leovy, J.C. Gille, and P.L. Bailey, Quasi-stationary zonally asymmetric circulations in the equatorial lower mesosphere, *J. Atmos. Sci., 44*, 2219–2236, 1987.

Holton, J.R., and H.-C. Tan, The influence of the equatorial quasi-biennial oscillation on the global circulation at 50 mb, *J. Atmos. Sci., 37*, 2200–2208, 1980.

Holton, J.R., and H.-C. Tan, The quasi-biennial oscillation in the Northern Hemisphere lower stratosphere, *J. Meteorol. Soc. Jpn., 60*, 140–148, 1982.

Labitzke, K., and H. van Loon, Association between the 11-year solar cycle, the QBO and the atmosphere. Part I: The troposphere and stratosphere in the northern hemisphere in winter, *J. Atmos. Terr. Phys., 50*, 197–206, 1988.

McIntyre, M.E., and T.N. Palmer, Breaking planetary waves in the stratosphere, *Nature, 305*, 593–600, 1983.

McIntyre, M.E., and T.N. Palmer, The 'surf zone' in the stratosphere, *J. Atmos. Terr. Phys., 46*, 825–849, 1984.

O'Sullivan, D.J., and T.J. Dunkerton, Seasonal development of the extratropical QBO in a numerical model of the middle atmosphere, *J. Atmos. Sci., 51*, 3706–3721, 1994.

Randel, W.J., The evaluation of winds from geopotential height data in the stratosphere, *J. Atmos. Sci., 44*, 3097–3120, 1987.

Robinson, W., The application of quasi-geostrophic Eliassen-Palm flux to the analysis of stratospheric data, *J. Atmos. Sci., 43*, 1017–1023, 1986.

Salby, M.L., Evidence of solar variability in the atmosphere: Its significance and relationship to terrestrial variability, in *The Solar Cycle Variation of the Stratosphere. A STEP Working Group 5 Report*, 16 pp., edited by L. Hood, Lunar and Planetary Laboratory, Department of Planetary Sciences, University of Arizona, 1995.

Salby, M.L., P. Callaghan, and D. Shea, Interdependence of the tropical and extratropical QBO: Relationship to the solar cycle vs. a biennial oscillation in the stratosphere, *J Geophys. Res*, in press, 1997.

Tung, K.-K., and H. Yang, Global QBO in circulation and ozone, Part I: Reexamination of observational evidence, *J. Atmos. Sci., 51*, 2699–2707, 1994a.

Tung, K.-K., and H. Yang, Global QBO in circulation and ozone, Part II: A simple mechanistic model, *J. Atmos. Sci., 51*, 2708–2721, 1994b.

van Loon, H., and K. Labitzke, Association between the 11-year solar cycle and the atmosphere. Part IV: The stratosphere, not grouped by the phase of the QBO. *J. Clim., 3*, 827–837, 1990.

Zurek, R.W., G.L. Manney, A.J. Miller, M.E. Gelman, and R.M. Nagatoni, Interannual variability of the north polar vortex in the lower stratosphere during the UARS mission, *Geophys. Res. Lett., 23*, 289–292, 1996.

M.P. Baldwin and T.J. Dunkerton, Northwest Research Associates, PO Box 3027, Bellevue, WA, 98009-3027. (e-mail: mark@nwra.com, tim@nwra.com)

(Received December 11, 1996; revised July 11, 1997; accepted July 22, 1997.)